UDK 691.714:621.793.8:628.483
Original scientific article/Izvirni znanstveni članek

ISSN 1580-2949
Mater. Tehnol.

ASSESSMENT OF WEAR AND CORROSION RESISTANCE IN TiC AND WC COATINGS APPLIED TO AISI 1040 FORGED STEEL VIA ELECTROSPARK DEPOSITION

OCENA OBRABNE IN KOROZIJSKE ODPORNOSTI TANKIH PREVLEK NA OSNOVI TiC IN WC, NANEŠENIH S POSTOPKOM ELEKTRIČNEGA ISKRENJA NA ODKOVKE IZ JEKLA VRSTE AISI 1040

D. R. P. Rajarathnam[1], K. Sundaramurthy[2], M. Makesh[2], R. Meiyazhagan[2]

[1]Paavai Engineering College, Department of Mechatronics Engineering, Namakkal, India
[2]Paavai Engineering College, Department of Mechanical Engineering, Namakkal, India

Prejem rokopisa – received: 2024-09-03; sprejem za objavo – accepted for publication: 2024-11-19

doi:10.17222/mit.2024.1289

Electrospark deposition is a very efficient technique used to improve metallic material surfaces by applying ceramic coatings. This investigation employed the electrospark deposition approach to deposit titanium carbide and tungsten carbide coatings onto the surface of AISI 1040 forged steel. Subsequently, the coated surfaces were subjected to a microstructure examination, phase structure analysis, microhardness testing, friction testing, wear testing, and electrochemical corrosion testing. After that, the outcomes were compared to those of uncoated AISI 1040 forged steel. The forged steel with TiC and WC phase coatings applied with electrospark deposition was much better than the untreated AISI 1040 forged steel in terms of hardness, being more than four times harder. Both the friction coefficient and wear volume loss were reduced as a result. Furthermore, due to their decreased conductivity, the ceramic coatings that were applied to the surface showed a corrosion resistance that was 2–3 times higher than that of the uncoated forged steel. While TiC coatings may better enhance corrosion resistance, this study provides evidence that WC coatings could be a superior choice for improving the wear resistance of AISI 1040 forged steel.

Keywords: electrospark deposition, ceramics, forged, hardness, metallic material, resistance, corrosion, coatings

Postopek nanašanja trde prevleke s postopkom električnega iskrenja (ESD; angl.: Electrospark deposition) je zelo učinkovita tehnika nanašanja tankih keramičnih plasti na površino kovinskih materialov z namenom izboljšanja njihove korozijske in obrabne odpornosti. V tem članku avtorji opisujejo raziskavo v kateri so uporabili ESD postopek za nanašanje prevlek na osnovi titanovega karbida (TiC) in volframovega karbida (WC) na površino kovanega jekla vrste AISI 1040. Po nanašanju keramičnih plasti so avtorji izvedli mikrostrukturne preiskave, fazno mikrostrukturno analizo, meritve mikrotrdote, testiranje trenja in obrabe ter elektro-kemijsko testiranje na odpornost proti koroziji. Sledila je primerjava med kovanim jeklom, ki ni imelo nanešene prevleke in jekloma s nanešeno TiC oz. WC prevleko. Kovano jeklo AISI 1040, ki je imelo TiC ali WC prevleko izdelano z ESD postopkom je imelo mnogo boljše lastnosti kot osnovno kovano jeklo brez prevleke. Koeficient trenja in odpornost proti obrabi sta se precej izboljšana. Nadalje, zaradi zmanjšanja električne prevodnosti površine se je odpornost proti koroziji povečala za 2 do 3-krat. Čeprav prevleka na osnovi TiC ima določene prednosti, ki se nanašajo na večjo odpornost proti koroziji je ta študija pokazala, da ima tudi prevleka iz WC svoj potencial glede izboljšanja odpornosti proti obrabi izbranega kovanega jekla vrste AISI 1040.

Ključne besede: nanašanje tankih plasti s pomočjo postopka električnega iskrenja, keramika, odkovki, trdota, kovinski material, obrabna in korozijska odpornost, prevleke

1 INTRODUCTION

AISI 1040 steel is widely used in numerous industries due to its strength and machinability, especially in moderate wear applications. In abrasive settings, gears, shafts, and rollers in the agricultural and sugarcane industries require durability. Crankshafts, axles, and couplings in the automotive and equipment industries use AISI 1040 to resist cyclical load and wear. This work uses TiC and WC coatings to improve AISI 1040's wear and corrosion resistance, potentially boosting component durability in challenging environments, extending service life and reducing maintenance.

Forged steels are highly valued in the automobile sector, particularly in the vehicle engines and powertrains of automobiles, due to their exceptional performance. Forged steels demonstrate the ability to remove metal efficiently at elevated cutting speeds, maintaining significant hardness over extended periods, even at high temperatures. This is achieved through the addition of varying amounts of alloy elements. Due to their exceptional hardness, strength, and affordability, they are highly favoured in the tool industry.[1] Nevertheless, their brittleness imposes certain restrictions on their application in situations involving significant impact forces and fatigue.[2]

*Corresponding author's e-mail:
drprajamala@gmail.com (D. R. P. Rajarathnam)

The surface of a material is often the starting point for corrosion and wear.[3] In order to mitigate these damages, one can utilize alloying techniques involving several elements or implement heat treatment methods. Nevertheless, the exorbitant expenses associated with these procedures make it more cost-effective to employ regional coating techniques with stronger materials of varying compositions to prolong the lifespan of the parts. Electrospark deposition (ESD) is a widely utilized method in both coating applications and the repair industry, due to its advanced technology and microwelding abilities.

Its application is limited, especially in decorative areas, due to uneven, rough surface structures resulting from ESD coating, the inability to control the thickness of the coating layer,[4] and the development of fissures caused by the differing thermal expansion properties of the electrode-coated material. Conversely, the main reasons for its preference are its ability to be conducted on-site, its energy efficiency,[5] its prevention of thermal degradation due to low heat input,[6] and its preservation of the coated material's metallurgical characteristics.[7]

The electrostatic discharge (ESD) approach is a micro-bonding method that makes use of short electrical pulses with high current in order to attach the electrode material to the metallic substrate. A small amount of thermal input is required for this method. It is important to note that although this method is comparable to pulsed micro-arc welding, it is different from it because of its use of brief electrical pulses.[8] A replacement electrode, an applicator that holds the electrode (either rotatable or rigid, based on the user's requirement), and an electric power source that includes a capacitor are the components of the system. During the operation of the system, the electrode performs the role of the anode, while the workpiece that is going to be coated represents the cathode. Coating uses the electrical current created by the capacitor discharge from the anode to cathode. After their separation from the electrode, droplets move in the direction of the workpiece, where they adhere to it through the process of mass transfer.

For a brief period of time, electrical pulses with high current and low voltage are utilized.[9] During electrostatic discharge (ESD), the material may occasionally solidify very quickly, which may result in the production of a nanocrystalline or amorphous structure. This is due to extremely rapid cooling rates of 105–106 *?* per second. Enhanced hardness, tribological properties, and resistance to corrosion are some of the benefits of this process.[10,11] In this experiment, the AISI 1040 forged steel surface was covered with titanium carbide and tungsten carbide using the ESD method. Through wear and electrochemical corrosion studies, the microscopic characteristics of the coated surface were identified, and the material properties were thoroughly examined in relation to the coating's impact.

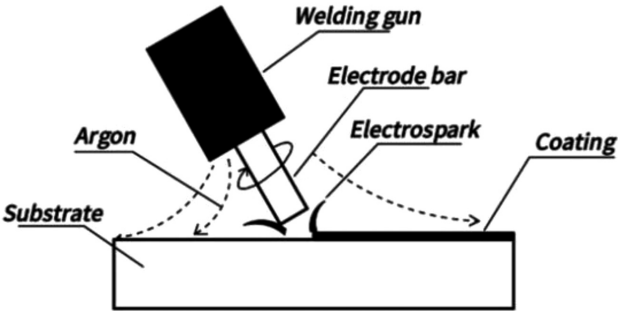

Figure 1: Visual depiction of the coating process

AISI 1040 forged-steel coatings including titanium carbide (TiC) and tungsten carbide (WC) were chosen for their wear resistance, notably in sugarcane-related abrasion and erosion. TiC adds hardness and chemical stability to steel's wear resistance in harsh environments, while WC's high melting point and low reactivity provide toughness and endurance. These coatings should improve steel's durability and performance, making it better for harsh industrial applications.

Wear rates were obtained using the track width, as per the equation given below.

$$\text{Wear rate } (\text{mm}^3/\text{Nm}) = \text{=worn volume } (\text{mm}^3)/\text{load (N)} \times \text{distance (m)} \quad (1)$$

2 EXPERIMENTAL STUDIES

AISI 1040 forged steel with a Ø16 mm and a length of 10 mm was utilized for the metallographic tests after being polished to a smoothness of 1200 grit. After the application of a coating, the samples were sliced at a right angle to the coating layer. After that, they were sanded with a substance with a grit of 1200, polished with a paste of alumina with a thickness of 1 μm, and then etched using the initial solution, which contained 3 % acid. The coating apparatus was a Huys 630 electrostatic discharge (ESD) device.

The parameters utilized for all the coatings were as follows: a frequency of 155 Hz, a voltage of 55 V, a capacitance of 160 μF, a rotation speed of 140 min^{-1} for the electrode, and a rotational speed of 140 min^{-1} for the substrate material. **Figure 1** is a depiction of the coating process. Using a scanning electron microscope (SEM), model LEO 1430 VP, various analyses were conducted, including capturing images of the coating layer, surface photos taken after the corrosion tests, measuring the thickness of the layers, and elemental analyses using EDX. The hardness of the layers was assessed using a microhardness tester (HMV-2) supplied by Shimadzu, applying a load of 50 g. The average value of 5 readings was recorded.

The Shumadzu XRD-6000 apparatus was utilized in order to perform an X-ray diffraction analysis on the phases produced on the coated surfaces. The wear test was carried out using a ball-on-disc system, under dry conditions, and at the temperature that was considered to be ambient. The test utilized a WC-Co ball with a diame-

ter of Ø8 mm, a wear rate of 0.3 m/s, a force of 6 N, and a distance of 260 m. In order to quantify the wear regions, the wear on the tribotechnic device, measured in terms of its cross-sectional extent, built by NANOVEA, was measured. Studies on electrochemical corrosion, namely potentiodynamic polarization, were carried out with the help of a Gamry Reference 600 galvanostat apparatus and the Echem Analyst software application.

At a temperature that was considered normal, the experiments were carried out in a liquid solution that contained 3.5 % sodium chloride. The set-up consisted of three electrodes. During the experiment, a saturated calomel electrode was utilized as the reference electrode. Through the utilization of a potential range of +250 mV per Ecorr and a scanning rate of 1 mV c^{-1}, Tafel curves were successfully acquired. The corrosion rates were examined by applying Faraday's notion to the calculations. An extensive analysis of the resistance to polarization curves (LPR) was conducted to determine the polarization resistance (R_p). The computation of the corrosion rate, which was measured in millimeters per year, polarization resistance (R_p), and electrochemical rate of corrosion (measured in microamperes per square centimeter, $\mu A \times cm^{-2}$) was done accordingly following the standards established by ASTM G102-89.

3 RESULTS AND DISCUSSION

3.1 Microstructure of the ceramic coating

Detailed pictures of the coating's microstructure obtained from the coated AISI 1040 forged steel cross-section are shown in **Figure 2**. The images are accompanied by their elemental analysis using energy-dispersive X-ray spectroscopy (EDX). After reviewing **Figure 2**, the presence of alloying zones in both coating types becomes apparent. The coating layer transformation contains minuscule pores and fissures. There are numerous factors that contribute to the development of these imperfections. Given that the covering electrode material is composed of ceramics, the electrical conductance of the coating electrode material is relatively poor, despite the fact that the coated metal has a high electrical conductance.

The above is one of the limitations. It is possible that alloying is difficult to accomplish due to the electrode's poor electrical conductivity, which decreases its capacity to melt.[12] As a result of the differences in thermal expansion coefficients between the coated material and the electrode, microcracks grow rapidly, and micro-distortions occur during the solidification process.[13]

Table 1: Coating thickness and hardness of bare, TiC-coated and WC-coated forged steel

Values	Uncoated AISI 1040	TiC-coated sample	WC-coated sample
Coating layer (μm)	–	32	24
Hardness ($HV_{0.05}$)	450	1558	1322

Microcracks are particularly noticeable during the solidification process. The application with multiple passes is necessary for ESD coating, and the most efficient coating is achieved when it is applied in three passes.[14,15] The ESD process is a technique that involves immediate heating and swift cooling. Furthermore, if the liquid electrode material does not fully solidify when it reaches the substrate surface, pulse discharge takes place. Thermal stress is heightened by this.[16] Given that defects primarily occur in the transition zone between the matrix and coating, it is clear that their creation is more pronounced

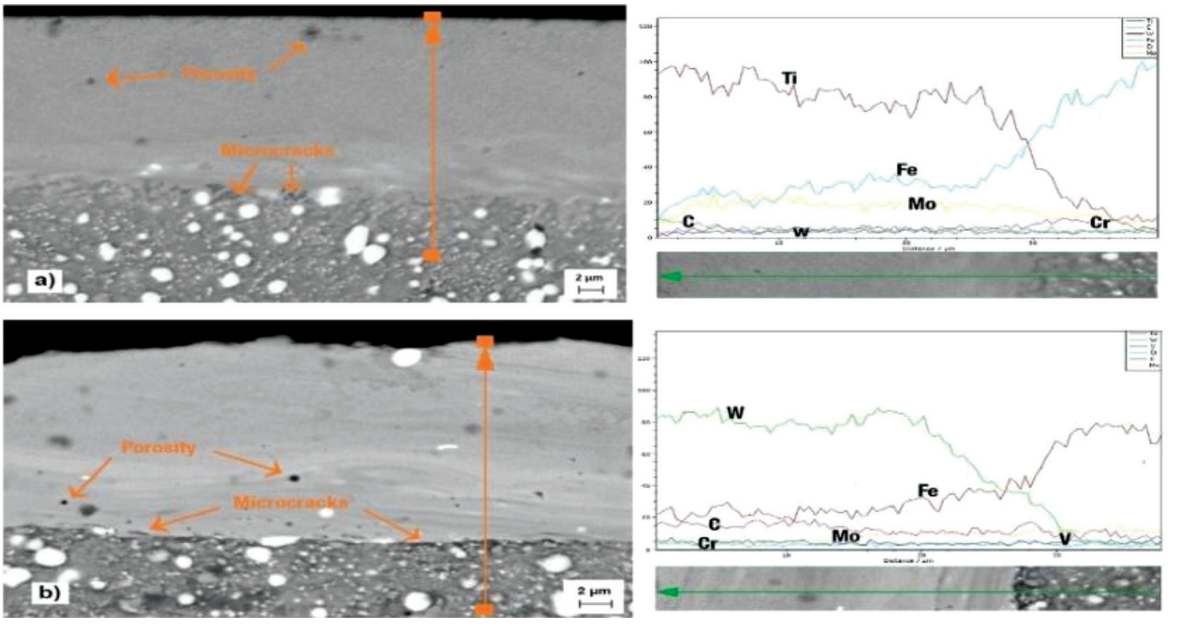

Figure 2: EDX pictures of coated AISI 1040 forged steel: a) titanium carbide, b) tungsten carbide

during the first application of the coating. Specifically, this is due to the fact that the thermal expansion coefficient and the electrical conductivity coefficient are significantly different in this particular area.

The above was the reason for our observation of this area. The differences in coefficients become less substantial as we rise to higher elevations, which leads to a reduction in the number of errors that need to be corrected. Specifically, this is due to the fact that lower coating passes use electrodes that are combined with the matrix material. The coating thickness and surface hardness presented in **Table 1** reveal that the coating that was applied using TiC had a layer thickness of 32 µm, whereas the coating that was applied using WC had a layer thickness of 24 µm. It was observed, by assessing the change in the hardness of the coating layer, that the surface hardness of AISI 1040 forged steel increases with the application of the coating, and is comparable to the behavior of the coating methods used in the past.[17] The AISI 1040 forged steel hardness is 450 $HV_{0.05}$. When coated with WC, the surface hardness is 1322 $HV_{0.05}$, and when coated with TiC, it is 1558 $HV_{0.05}$. Several variables influence the surface hardness of an ESD coating. Due to the ceramic composition of the composite coating electrodes (WC and TiC), it is anticipated that the coating results in an increase in the surface hardness of the material. In addition, it is essential to consider the fact that the combination of components in the electrode and the substance being coated has a positive impact on the degree of coating hardness. When alloy components precipitate or dissolve in solid solutions, structural hardening is likely to result in an increased hardness. This occurs as a result of the disintegration of the components of the alloy. During the coating, the particles become detached from the electrode and form a bond or merge with the substance. The rapid cooling that occurs during this phase results in the formation of metastable structures during the solidification. These structures improve the solid solution and lead to an increase in its hardness.[18] **Figure 3** illustrates the X-ray diffraction pattern of AISI 1040 forged steel that was coated with electrodes made of titanium carbide and tungsten carbide using the electrospark deposition (ESD) technology.

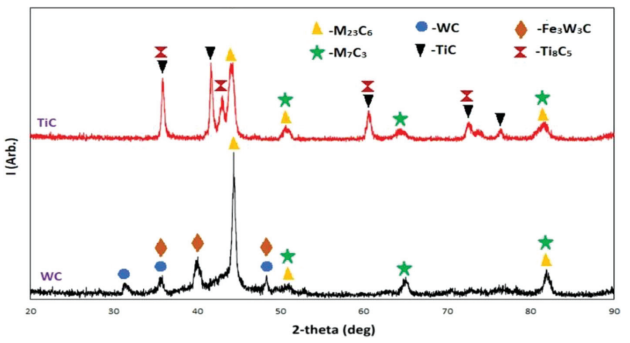

Figure 3: XRD patterns of ESD-formed TiC and WC coating

Analysing **Figure 3**, it is discovered that the coating that was created using the WC electrode displays peaks on the surface morphology that correlate to the Fe_3W_3C phase and WC phase. On the other hand, the coating that was produced using the TiC electrode has prominent peaks that correspond to the TiC phase and Ti_8C_5 phase. During the coating, particles composed of tungsten (W), titanium (Ti), and carbon (C), which separate from the electrode, can be found adhering to the surface of the material. These particles then begin to scatter, forming alloys with the elements that are already present in the substrate material.[19,20] This is indicated by the peaks that correspond to various carbide compounds present in the coating. The resistance to wear, corrosion resistance, and the material surface hardness are all improved by these phases, which are characterized by a more stable structure. Finally, the chemical composition of AISI 1040 forged steel includes the $M_{23}C_6$ phase, which is composed of chromium (Cr) and iron (Fe). This phase is evident in the pronounced peaks of both coatings.

Other peaks correspond to the M_7C_3 phase. Typically, this circumstance can be elucidated using two distinct explanations. An alloy is formed due to the combination of the electrode material and coated material. Conversely, the ESD coating is performed by hand. The surface morphology of the coatings produced with this method is inherently challenging to regulate and lacks uniformity across the whole layer. Prior research revealed that after three coatings, there is no further increase in the mass transfer and coating layers. Thus, the X-ray diffraction (XRD) pattern of an electrostatic discharge (ESD) coating might be influenced by the metal coated surface due to the presence of intermittent spaces between the splashes.

Electrospark deposition (ESD) can deposit TiC and WC coatings due to a strong metallurgical bonding; however, this method also has limits. The coating thickness is minimal, which may not be enough for long-term high-wear applications. ESD may cause irregular coating thickness and residual strains or microcracks in the coating layer, compromising its wear and corrosion resistance under certain operational conditions. These variables are essential for a coating durability and efficacy evaluation.

3.2 Tribological behavior

The wear test provided the wear rate and friction coefficient graph shown in **Figure 4a**. The uncoated AISI 1040 wear rate is shown in **Figure 4b**. **Figure 4c** illustrates the wear that occurs on AISI 1040 that was forged and covered with the TiC electrode. **Figure 4d** illustrates the wear that occurs on forged steel coated with the WC electrode. The wear rates and friction coefficients of the uncoated sample, the samples coated with TiC and WC were found to be 227 × 10^{-6}, 183 × 10^{-6}, and 89 × 10^{-6} mm^3/Nm, respectively, as depicted by the graph in **Fig-**

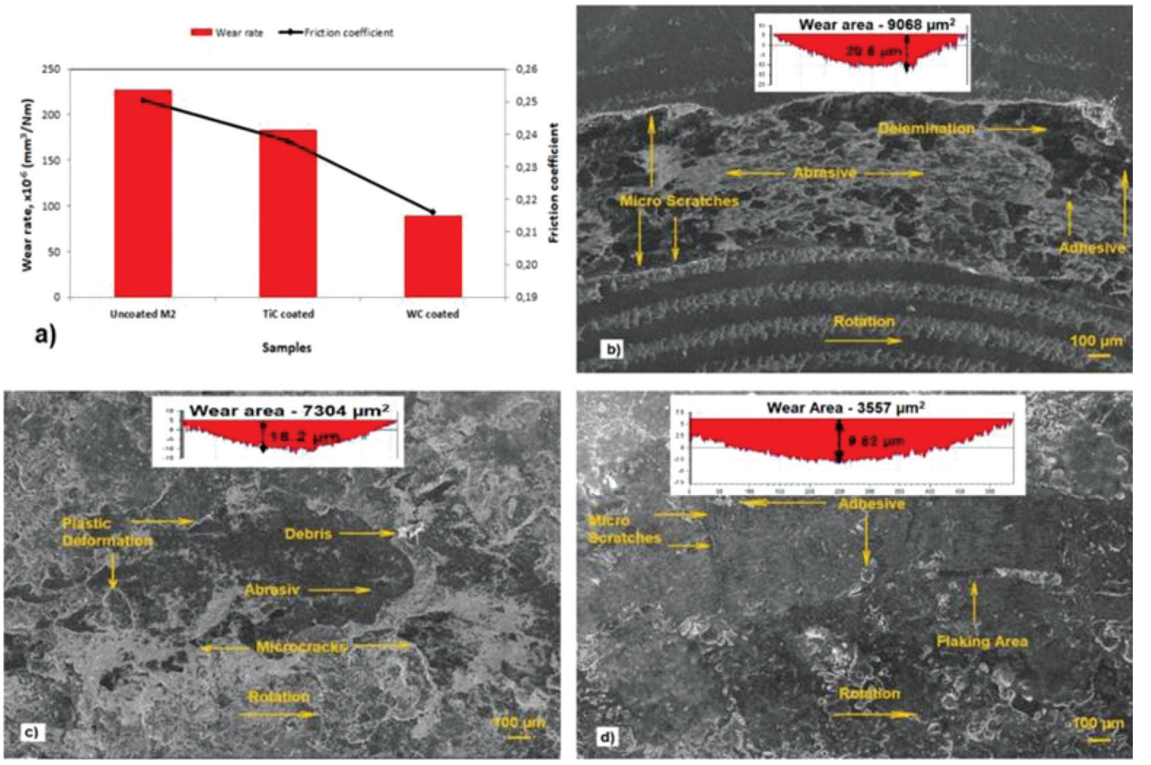

Figure 4: a) Graph depicting the relationship between the wear rate and coefficient of friction. SEM pictures of the wear markings of b) uncoated steel, c) coated with titanium carbide and d) coated with tungsten carbide

ure 4a. The AISI 1040 forged steel sample that was left uncoated had the highest wear rate and friction coefficient, whereas the sample coated with WC had the lowest values.

Figures 4b to **4d** present the wear zone and scar penetrations observed with scanning electron microscopy (SEM) after the dry environment wear test. Using surface scanning, the wear zone and scar penetrations of the uncoated AISI 1040 forged steel, and the samples coated with TiC and WC were found to be 99.068 mm^2 – 20.6 µm, 7.304 mm^2 – 18.2 µm, and 3.557 mm^2 – 9.82 µm, respectively. The coating layer is higher than the track depths. The uncoated AISI 1040 forged steel has the highest values for the wear region and scar depth, while the WC-coated AISI 1040 forged steel has the lowest values.

It is clear from the SEM photographs of the wear markings that both abrasive and adhesive wear were found on the uncoated sample after performing the wear test in dry condition. Furthermore, it is evident that the abrasive ball is the source of delamination and microscratches. There are abrasive wear types, microcracks, deformation zones, and shattered particles in the TiC coating. The most common type of wear in the WC coating is adhesive wear. Furthermore, it is evident that there are flaking patches and localized microscratches. Despite the fact that the titanium carbide-coated sample has a higher hardness than the tungsten carbide-coated sample, it is discovered that the wear rate of the WC coating is reduced. Because of the tougher nature of the TiC coating, the layer exhibits brittle behavior. The surface exhibits its plastic deformation as a result of the particles in the coating breaking off from fatigue under repeated stresses. Nonetheless, mechanical stresses are caused by Hertz forces that exist in the contact area. Particles separate from the material more readily when critical limit values are exceeded because this leads to the creation and distribution of cracks on hard surfaces.[21,22] This explains why, despite having a larger layer thickness and microhardness, the wear rate of the TiC-coated sample is lower.

Due to tungsten carbide's high hardness and fracture toughness, WC coatings resist abrasion. For applications involving physical abrasion, WC's powerful covalent bonds make them durable under high stress. Titanium carbide's chemical stability and inertness make TiC coatings very corrosion resistant. This stability reduces oxidation and corrosion, especially in acidic or high-humidity conditions, making the substrate more corrosion resistant. Each coating's chemical and structural features, tailored for industrial challenges, define its performance.

Table 2: Electrochemical corrosion test values for coated and uncoated AISI 1040

AISI 1040	E_{cor} (mV)	I_{cor} (µA)	Rate of corrosion (MPY)	R_p (kΩ)
Uncoated	–460	57.50	11.40	0.165
coated WC	–514	24.50	6.240	1.15
coated TiC	–455	16.00	3.667	7.95

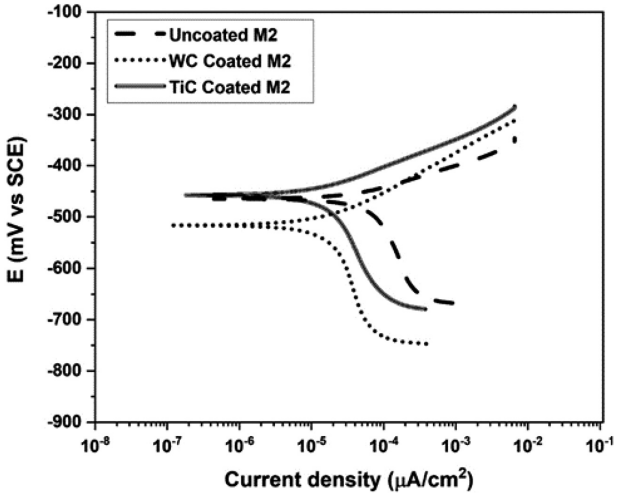

Figure 5: Representation of Tafel curves

3.3 Electrochemical corrosion analysis

Table 2 presents the results of the electrochemical corrosion test, conducted at room temperature on both uncoated and ESD-coated AISI 1040 forged steel, using TiC and WC electrodes. Their Tafel curves are shown in **Figure 5.**

Figure 6 displays scanning images of the surfaces and EDX findings of the corrosion test.

When analyzing **Table 2** and **Figure 5**, it is clear that while the Ecor values of the TiC-coated and uncoated samples are similar, the WC values show a stronger negative correlation. For the uncoated AISI 1040 forged steel, and the samples coated with WC and TiC, the corresponding Icor values were found to be 57.60 μA, 24.00 μA and 17.00 μA. Coating caused a drop in the Icor values. In comparison with the uncoated sample, the corrosion resistance increased two to three times. Fissures can be seen in the SEM images (**Figure 6**), showing the surfaces of the specimens coated with TiC and WC that were acquired after the corrosion test.

The Cl- ions in the NaCl solution exhibit a very aggressive behavior, attempting to penetrate surface fissures in order to reach the matrix. This ultimately results in metastable pitting corrosion in the affected areas. These ions are also responsible for initiating pitting and cathodic reduction of oxygen, referred to as the OH-formation. However, the layers of ceramic coating developed on the surface are another factor contributing to the increased corrosion resistance due to the fact that these materials are less conductive than steel.[23–24]

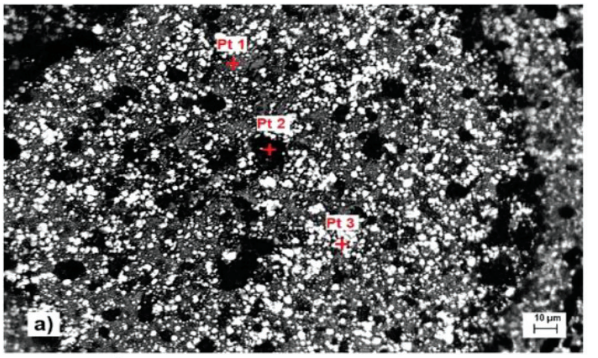

Pt/Elt	C	V	Cr	Fe	Mo	W	Cl	Na
1	16.8	1.7	5.5	71.1	2.5	1.6	0.8	3.1
2	20.5	1.3	1.9	55.5	1.9	2.1	8.9	10.2
3	28.7	2.7	4.2	52.9	2.3	34	1.1	2.7

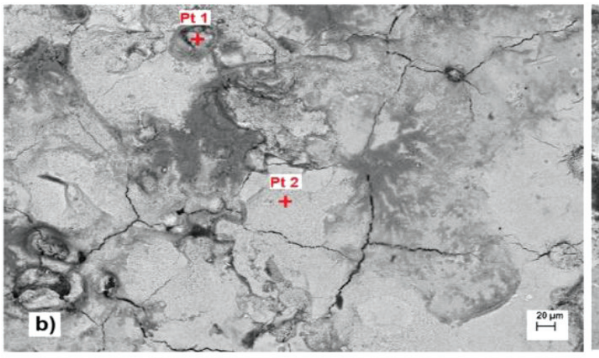

Pt/Elt	C	V	Cr	Fe	Mo	W	Cl	Na	Ti
1	17.9	1.7	1.7	20.2	3.2	0.5	5.4	15.5	27.9
2	31.3	1.8	3.2	13.6	4.5	0.7	0.3	1.1	39.0

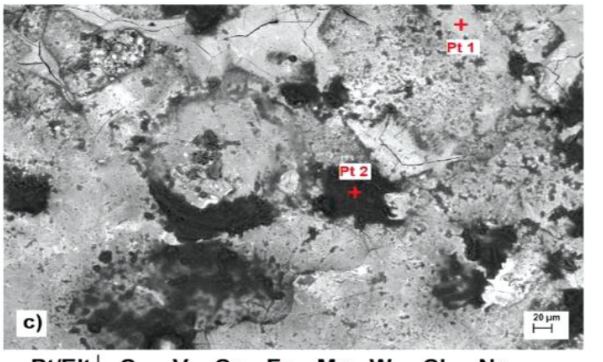

Pt/Elt	C	V	Cr	Fe	Mo	W	Cl	Na
1	22.1	1.3	3.1	61.0	1.9	9.2	1.2	5.1
2	4.2	0.4	0.2	6.1	0.2	1.7	36.9	41.6

Figure 6: Corrosion test results for AISI 1040 steel: a) uncoated, b) coated with TiC, and c) coated with WC

As the Icor values of the coated samples are lower than that of the uncoated sample, it may be concluded that even though local corrosion originated in these areas and spread throughout the material, the cracks did not extend into the matrix. The surface exhibits cracks as a result of high tensile load caused by its incompatibility with the heat between successive runs.[25] The absence of fissures between passes in the cross-sectional microstructure images further confirms that corrosion is confined to the bottom coating layer and does not reach the matrix (**Figure 2**).

The following are the electrochemical processes that take place in a 3.5 % NaCl solution for TiC and WC:

$$TiC + O_2 \rightarrow Ti + CO_2 \quad (2)$$

$$2H_2O + O_2 + 4e^- \rightarrow 4OH^- \quad (3)$$

$$3Ti + 2O_2 + 4OH^- \rightarrow 3TiO_2 + 2H_2O + 4e^- \quad (4)$$

$$WC + 5H_2O \rightarrow WO_3 + CO_2 + 10H + 10e^- \quad (5)$$

$$2H_2O + O_2 + 4e^- \rightarrow 4OH^- \quad (6)$$

These reactions lead to the formation of TiO_2 and WO_3 compounds as corrosion products. When WC and NaCl interact, WC oxidizes in the solution. In contrast, TiC reacts with NaCl to generate a persistent and protective layer of TiO_2 at the interface.[26] This is an additional indication of the TiC-coated sample's exceptional corrosion resistance.

Electrochemical stability of each element in the material must be taken into account during corrosion resistance assessments. Consequently, the influence of $M_{23}C_6$ and M_7C_3 (M = Cr, Fe) is identified.

We cannot ignore the phases present on the surfaces as a consequence of amalgamation that takes place during coating, as shown by the XRD coating patterns (**Figure 3**). This is because corrosion resistance is the only factor that can be considered. Cr is more resistant to corrosion than Fe is, and when exposed to acidic aqueous electrolytes, Fe and Cr oxidize to generate Fe_2O_3, Fe_3O_4, Cr_2O_3, and Cr_2O_3, resulting in the formation of a passive coating on the surface and contributing to a reduction in corrosion.[27] However, when comparing the bare steel, WC-coated and TiC-coated AISI 1040 forged steel, the resistance to corrosion (R_p) and rate of corrosion of these materials were as follows: 0.165 kΩ – 11.40 MPY, 1.15 kΩ – 6.240 MPY, and 7.95 kΩ – 3.667 MPY, respectively.

It is evident that corrosion resistance increases with coating since coated samples have stronger corrosion resistance and lower corrosion rates. Excellent corrosion potential and low corrosion current are regarded as the indicators of a material's excellent corrosion resistance.[28,29] Through the utilization of the ESD methodology, it becomes apparent that the resistance to corrosion of TiC-coated and WC-coated specimens increases as the rate of corrosion decreases.

4 CONCLUSIONS

TiC-coated AISI 1040 forged steel is ideal for chemical processing, maritime engineering, and oil and gas industries that require corrosion resistance. In these environments, TiC's corrosion resistance improves equipment life and reduces maintenance costs. However, mining, construction, and the sugarcane industry use WC-coated steel for wear resistance under high mechanical forces. With continual impacts and friction, cutting tools, mill rolls, and wear plates benefit from WC coatings' durability and abrasion resistance. These diverse applications highlight the coatings' adaptability across various sectors and environmental issues.

The following are the outcomes of applying TiC and WC electrodes to the AISI 1040 forged steel surface via the ESD technique:

Using the ESD method, TIC and WC electrodes were successfully applied to the AISI 1040 forged steel surface.

The layer of coating contains small porosities and has a homogeneous, uniform, and continuous structure.

The XRD patterns of the coating layers revealed the phases present: Fe_3W_3C, $M_{23}C_6$, and M_7C_3 for the TiC coating, and WC, TiC, Ti_8C_5, $M_{23}C_6$, and M_7C_3 for the WC coating.

The wear rate and coefficient of friction of the AISI 1040 forged steel coated with TiC and WC were reduced; however, the WC coating exhibited a lower wear value. The TiC coating was most effective in reducing the wear rate.

The corrosion test results show that Ecor values were quite close to one another, with the WC-coated AISI 1040 forged steel having the lowest value.

Icor values drop with the coating. The values that exhibit this trend is as follows: uncoated AISI 1040 > WC-coated steel > TiC-coated steel.

In corrosive environments, a coating or substrate material deteriorates at a reduced pace, hence improving corrosion resistance. Protective coatings such as TiC or WC safeguard steel for prolonged durations, maintaining mechanical strength and surface integrity. The relationship between corrosion rate and resistance affects a component's longevity in sectors such as chemical processing and sugarcane industry, where exposure to aggressive chemicals or moisture is prevalent. Significantly, the TiC coating, applied using the ESD approach, demonstrates the greatest corrosion resistance and a minimal corrosion rate.

Acknowledgement

The research was supported by my father, Mr. D. Ponnusamy, and my spouse, Mrs. B. Malathi. I wish to extend special thanks to Professor Dr. K. K. Ramasamy and Dr. M. Premkumar from the Paavai Engineering College, Namakkal, India, for their valuable help.

5 REFERENCES

[1] D. Wang, L. Zhan, C. Liu, D. He, R. Lai, Y. Li, Q. Zeng, Stress-level dependency of creep ageing behavior for the nugget zone in a friction stir welded Al–Cu–Li alloy, Mater Sci Eng, 881 (**2023**), 1–13

[2] P. Jovičević-Klug, G. Puš, M. Jovičević-Klug, B. Žužek, B. Podgornik, Influence of heat treatment parameters on effectiveness of deep cryogenic treatment on properties of high-speed steels, Mater Sci Eng A, 829 (**2022**), 1–12

[3] U. Mishigdorzhiyn, A. Semenov, N. Ulakhanov, A. Milonov, D. Dasheev, P. Gulyashinov, Microstructure and wear resistance of hot-work tool steels after electron beam surface alloying with B4C and Al, Lubricants, 10 (**2022**) 5,1–17

[4] Y. Kayali, Y. Yaląin, Ş. Talaş, Electro-spark deposition coating of AISI 4140 and AISI 1040 steels by WC, Ni and M42 electrodes and their wear properties, J Mater Eng Perform, 33 (**2023**), doi: 10.1007/s11665- 023-08794-5

[5] C. Barile, C. Casavola, G. Pappalettera, G. Renna, Advancements in electrospark deposition (ESD) technique: A short review, Coatings, 12 (**2022**), 1–28

[6] Y. Kayali, E. Kanca, A. Günen, Effect of boronizing on microstructure, high-temperature wear and corrosion behavior of additive manufactured Inconel 718, Mater Charact, 191 (**2022**), 1–17

[7] E. Mertgenc, S. Talas, B. Gokce, The wear and microstructural characterization of copper surface coated with TiC reinforced FeAl intermetallic composite by ESD method, Mater Res Express, 6 (**2019**), 1–10

[8] Y. J. Xie, M. C. Wang, Microstructural morphology of electrospark deposition layer of a high gamma prime superalloy, Surf Coat Technol, 201 (**2006**), 691–8

[9] Z. Li, W. Gao, Y. He, Protection of a Ti3Al–Nb alloy by electrospark deposition coating, Scr Mater, 45 (**2001**), 1099–1105

[10] M. Brochu, J. G. Portillo, J. Milligan, D. W. Heard, Development of metastable solidification structures using the electrospark deposition process, Open Surf Sci J, 3 (**2011**),105–14

[11] P. Leo, G. Renna, G. Casalino, Study of the direct metal deposition of AA2024 by electrospark for coating and reparation scopes, Appl Sci (Switz), 7 (**2017**), 1–16

[12] O. Demirbilek, M. Onan, N. Unlu, S. Talas, Investigation of the efficiency for ESD coating with stainless steel on die surfaces, Int J Surf Sci Eng, 16 (**2022**), 335–48

[13] Y. Kayali, M. C. Yaląin, A. Buyuksagis, Effect of electro spark deposition coatings on surface hardness and corrosion resistance of ductile iron, Can Metall Q, 62 (**2023**), 483–96

[14] K. Korkmaz, Investigation and characterization of electrospark deposited chromium carbide-based coating on the steel, Surf Coat Technol, 272 (**2015**), 1–7

[15] M. Fakoori Hasanabadi, F. Malek Ghaini, M. Ebrahimnia, H. R. Shahverdi, Production of amorphous and nanocrystalline iron based coatings by electro-spark deposition process, Surf Coat Technol, 270 (**2015**), 95–101

[16] W. Wang, M. Du, X. Zhang, C. Luan, Y. Tian, Preparation and properties of Mo coating on H13 steel by electro spark deposition process, Materials,14 (**2021**), 1–15

[17] Y. Kayali, Y. Akcin, E. Mertgenc, B. Gokce, Investigation of kinetics of borided ductile and lamellar graphite cast iron, Prot Met Phys Chem Surf, 53 (**2017**),127–32

[18] J. Tang, Mechanical and tribological properties of the TiC-TiB2 composite coating deposited on 40Cr-steel by electrospark deposition, Appl Surf Sci, 365 (**2016**), 202–8

[19] Q. Xiao, W. lei Sun, K. xin Yang, X. feng Xing, Z. hao Chen, H. nan Zhou, Wear mechanisms and micro-evaluation on WC particles investigation of WC-Fe composite coatings fabricated by laser cladding, Surf Coat Technol, 420 (**2021**), 1–12

[20] J. Z. Lu, J. Cao, H. F. Lu, L. Y. Zhang, K. Y. Luo, Wear properties and micro-structural analyses of Fe-based coatings with various WC contents on H13 die steel by laser cladding, Surf Coat Technol, 369 (**2019**), 228–37

[21] H. Cimenoglu, E. Atar, A. Motallebzadeh, High temperature tribological behaviour of borided surfaces based on the phase structure of the boride layer, Wear, 309 (**2014**),152–8

[22] M. S. Gok, Y. Kuauk, A. Erdogan, M. Oge, E. Kanca, A. Gunen, Dry sliding wear behavior of borided hot-work tool steel at elevated temperatures, Surf Coat Technol, 328 (**2017**), 54–62

[23] S. Bilgin, O. Guler, U. Alver, F. Erdemir, M. Aslan, A. Canakci, Effect of TiN, TiAlCN, AlCrN, and AlTiN ceramic coatings on corrosion behavior of tungsten carbide tool, J Aus Ceram Soc, 57 (**2021**), 263–73

[24] H. Wang, H. Lu, X. Song, X. Yan, X. Liu, Z. Nie, Corrosion resistance enhancement of WC cermet coating by carbides alloying, Corros Sci, 147 (**2019**), 372–83

[25] Q. Zhang, N. Lin, Y. He, Effects of Mo additions on the corrosion behavior of WC-TiC-Ni hardmetals in acidic solutions, Int J Refract Met Hard Mater, 38 (**2013**), 15–25

[26] B. Han, S. Zhu, W. Dong, Y. Bai, H. Ding, Y. Luo, Improved mechanical performance and electrochemical corrosion of WC-Al2O3 composite in NaCl solution by adding the TiC additives, Int J Refract Met Hard Mater, 99 (**2021**), 1–13

[27] A. Parakh, M. Vaidya, N. Kumar, R. Chetty, B. S. Murty, Effect of crystal structure and grain size on corrosion properties of AlCoCrFeNi high entropy alloy, J Alloy Compd, 863 (**2021**), 1–10

[28] H. R. Bakhsheshi-Rad, E. Hamzah, A. F. Ismail, M. Daroonparvar, M. A. M. Yajid, M. Medraj, Preparation and characterization of NiCrAlY/nano-YSZ/PCL composite coatings obtained by combination of atmospheric plasma spraying and dip coating on Mg-Ca alloy, J Alloy Compd, 658 (**2016**), 440–52

[29] J. Sun, Q. G. Fu, L. P. Guo, Y. Liu, C. X. Huo, H. J. Li, Effect of filler on the oxidation protective ability of MoSi2 coating for Mo substrate by halide activated pack cementation, Mater Des, 92 (**2016**), 602–9